

Formation of Rust During the Corrosion of Steel in Water and (NH₄)₂SO₄ Solutions

Musić, Svetozar; Dragičević, Dragica; Popović, Stanko

Source / Izvornik: **Croatica Chemica Acta, 1993, 66, 469 - 478**

Journal article, Published version

Rad u časopisu, Objavljena verzija rada (izdavačev PDF)

Permanent link / Trajna poveznica: <https://um.nsk.hr/um:nbn:hr:217:226998>

Rights / Prava: [In copyright](#) / [Zaštićeno autorskim pravom.](#)

Download date / Datum preuzimanja: **2024-04-25**



Repository / Repozitorij:

[Repository of the Faculty of Science - University of Zagreb](#)



Formation of Rust During the Corrosion of Steel in Water and $(\text{NH}_4)_2\text{SO}_4$ Solutions

Svetozar Musić^{a,*}, Đurđica Dragčević^a and Stanko Popović^b

^a Ruđer Bošković Institute, P. O. Box 1016,
41001 Zagreb, Republic of Croatia

^b Department of Physics, Faculty of Science, University of Zagreb,
P. O. Box 162, 41001 Zagreb, Republic of Croatia

Received May 25, 1993

Formation of rust during the corrosion of steel in water and $(\text{NH}_4)_2\text{SO}_4$ solutions was monitored at 20 °C up to 3 months and at 90 °C up to 3 days. All corrosion products were analyzed by X-ray diffraction and Fourier transform IR spectroscopy. Four oxide phases, lepidocrocite ($\gamma\text{-FeOOH}$), goethite ($\alpha\text{-FeOOH}$), magnetite (Fe_3O_4) and hematite ($\alpha\text{-Fe}_2\text{O}_3$), were found in the corrosion products. Their distribution or absence of some oxide phases in corrosion products were strongly dependent on the experimental conditions. The strong influence of $(\text{NH}_4)_2\text{SO}_4$ electrolyte on the phase composition of the rust was explained by the cumulative effect of two aggressive ions, NH_4^+ and SO_4^{2-} . Possible pathways for the formation of iron oxide phases in the rust were discussed.

INTRODUCTION

The phase composition of the corrosion products of steel, formed in aqueous medium, depends on different factors, such as the electrolyte character of aqueous medium, temperature, pH, oxygen content as well as the nature of steel. Surface pretreatment of steel may also affect the phase composition of the corrosion products of steel. In the literature, there are abundant data about the phase composition of the rust formed by the corrosion of steel in aqueous medium. However, discrepancies concerning the chemical and structural properties of the rust are significant. Several factors are responsible for this, such as crystallinity, stoichiometry, particle size of oxide components in the rust, *etc.* Limitations of experimental techniques can also be a source of errors in determination of the phase composition of the rust. Finally, many researchers performed their experiments under poorly defined conditions.

* Author to whom correspondence should be addressed.

Numerous investigations showed the presence of different oxide phases in the rust, such as $\text{Fe}(\text{OH})_2$, amorphous $\text{Fe}(\text{OH})_3$, ferrihydrite, $\alpha\text{-FeOOH}$, $\beta\text{-FeOOH}$, $\gamma\text{-FeOOH}$, $\delta\text{-FeOOH}$, $\alpha\text{-Fe}_2\text{O}_3$, $\gamma\text{-Fe}_2\text{O}_3$ and Fe_3O_4 or $\text{Fe}_{3-x}\text{O}_4$. In previous papers, we showed that Mössbauer spectroscopy can be a very useful technique in the phase analysis of the rust formed by the atmospheric corrosion of steel¹ or by the corrosion of steel in aqueous medium.² The corrosion of steel in aqueous medium is a process of electrochemical nature and the generated rust is a mixture of different oxide phases exhibiting colloidal properties. The mechanism of rust formation during the corrosion of steel in aqueous medium can be followed, to a certain stage, by analogy to the precipitation of iron oxyhydroxides and oxides from $\text{Fe}(\text{II})$ - or $\text{Fe}(\text{III})$ -salt solutions.³⁻⁶ The usefulness of these investigations increases as the conditions in the laboratory experiments approach those in actual corrosion processes.

In the present paper, we report the results of the analysis of the corrosion products of steel formed in doubly distilled water and in $(\text{NH}_4)_2\text{SO}_4$ solutions. These experiments were performed in order to find out the influence of the $(\text{NH}_4)_2\text{SO}_4$ electrolyte and its concentration on the chemical and structural properties of the rust. X-ray diffraction (XRD) and Fourier transform infrared (FT-IR) spectroscopy were used as instrumental techniques. FT-IR spectroscopy is a technique that is characterized by a better sensitivity and resolution than conventional IR spectroscopy.

TABLE I
Experimental conditions for the preparation of the corrosion products of steel (samples C₁ to C₂₄)

Sample	Solution	Temperature of solution (°C)	Time of corrosion*	pH of mother liquor
C ₁	H ₂ O	20	1d	5.50
C ₂	H ₂ O	20	3d	5.35
C ₃	H ₂ O	20	7d	5.50
C ₄	H ₂ O	20	21d	5.40
C ₅	H ₂ O	20	3m	5.90
C ₆	H ₂ O	90	5h	7.78
C ₇	H ₂ O	90	1d	6.45
C ₈	H ₂ O	90	3d	6.35
C ₉	0.1 M $(\text{NH}_4)_2\text{SO}_4$	20	1d	7.15
C ₁₀	0.1 M $(\text{NH}_4)_2\text{SO}_4$	20	3d	7.45
C ₁₁	0.1 M $(\text{NH}_4)_2\text{SO}_4$	20	7d	7.35
C ₁₂	0.1 M $(\text{NH}_4)_2\text{SO}_4$	20	21d	7.40
C ₁₃	0.1 M $(\text{NH}_4)_2\text{SO}_4$	20	3m	7.70
C ₁₄	0.1 M $(\text{NH}_4)_2\text{SO}_4$	90	5h	7.45
C ₁₅	0.1 M $(\text{NH}_4)_2\text{SO}_4$	90	1d	7.35
C ₁₆	0.1 M $(\text{NH}_4)_2\text{SO}_4$	90	3d	7.50
C ₁₇	2 M $(\text{NH}_4)_2\text{SO}_4$	20	1d	7.85
C ₁₈	2 M $(\text{NH}_4)_2\text{SO}_4$	20	3d	7.90
C ₁₉	2 M $(\text{NH}_4)_2\text{SO}_4$	20	7d	8.25
C ₂₀	2 M $(\text{NH}_4)_2\text{SO}_4$	20	21d	8.05
C ₂₁	2 M $(\text{NH}_4)_2\text{SO}_4$	20	3m	6.80
C ₂₂	2 M $(\text{NH}_4)_2\text{SO}_4$	90	5h	8.00
C ₂₃	2 M $(\text{NH}_4)_2\text{SO}_4$	90	1d	7.95
C ₂₄	2 M $(\text{NH}_4)_2\text{SO}_4$	90	3d	8.00

* h = hour, d = day, m = month

EXPERIMENTAL

Ammonium sulphate *p. a.*, obtained by Kemika (Zagreb, Croatia) and doubly distilled water were used. Cold rolled low carbon steel, JUS-C0146 ($C_{\max} = 0.12\%$, $Mn_{\max} = 0.50\%$, $P_{\max} = 0.040\%$, $S_{\max} = 0.040\%$), was used. Commercial steel foil was cut into coupons with 60 mm x 100 mm dimensions. The steel coupons were polished and cleaned with doubly distilled water and ethanol. Experiments were performed at 20 or 90 °C. At 20 °C, glass beakers were covered hermetically with polyethylene foils to prevent direct contact of the corrosion system with atmospheric oxygen. In glass beakers, the steel coupons were completely immersed into the aqueous medium. Corrosion of steel at 90 °C was performed in an autoclave. Experimental conditions for the preparation of corrosion products of steel, C_1 to C_{24} , are given in Table I. Isolated corrosion products were cleaned from mother liquor with doubly distilled water. Sorvall RC2-B ultraspeed centrifuge (up to 20000 r.p.m.) was used for separation of the solid from the liquid phases. The corrosion products were dried in vacuum at room temperature. pH measurements were performed with a pHM-26 instrument and the corresponding electrodes produced by Radiometer. X-ray powder diffraction measurements were performed using a Phillips counter diffractometer with monochromatized $CuK\alpha$ radiation and graphite monochromator. FT-IR spectra were recorded using a 1720x spectrometer produced by Perkin-Elmer. FT-IR spectrometer was coupled with a personal computer loaded with IR Data Manager (IRDM) program. The samples were pressed into discs using spectroscopically pure KBr. The origin of standard iron oxides was described in a previous paper.⁴

RESULTS

Phase compositions of the corrosion products formed in doubly distilled water were strongly dependent on the temperature in the experiment. Table II shows the phase composition of the samples, determined by XRD. γ -FeOOH was the dominant component in samples C_1 to C_5 , which were obtained at 20 °C. Fe_3O_4 was an additional component in these samples and the content of Fe_3O_4 in the rust increased with prolonged time of corrosion. FT-IR spectra of samples C_1 to C_5 are shown in Figure 1. Sharp and very pronounced bands at 1024 and 745–750 cm^{-1} are typical of γ -FeOOH. In sample C_1 , Fe_3O_4 could be detected only on the basis of the shoulder at 549 cm^{-1} . As Fe_3O_4 content increased, the intensity of this shoulder also increased and it was shifted to 557 cm^{-1} for sample C_5 . In sample C_5 , a small amount of α -FeOOH was also detected by FT-IR, on the basis of bands of very small intensities at 893 and 801 cm^{-1} .

Corrosion of steel in doubly distilled water at 90 °C generated corrosion products in which Fe_3O_4 was the dominant component, while γ -FeOOH and α -Fe₂O₃ were additional components, as shown by XRD analysis (Table II). FT-IR spectra of samples C_6 to C_8 are shown in Figure 2. The Fe_3O_4 component could be detected only on the basis of a very strong band at 575–578 cm^{-1} . However, in the interpretation of these spectra we must keep in mind the fact that this IR band is a superposition of two bands corresponding to both Fe_3O_4 and α -Fe₂O₃. For this reason, a clear distinction between Fe_3O_4 and α -Fe₂O₃ in these samples was not possible only by FT-IR for the given range, 1400–370 cm^{-1} . The nature of IR bands, corresponding to iron hydroxides, oxyhydroxides, oxides and basic sulphates, was discussed in our previous papers,^{7–9} and will not be elaborated in the present paper. FT-IR spectra, shown in Figure 2, also indicated that the content of γ -FeOOH in the rust decreased from sample C_6 to sample C_8 . In sample C_8 , only a small amount of γ -FeOOH could be detected on the basis of a very weak peak at 1021 cm^{-1} . In sample C_6 , a small amount of α -FeOOH was detected on the basis of bands at 893 and 800 cm^{-1} . With a prolonged time of corrosion, the intensities of these bands were increased.

TABLE II

The result of XRD phase analysis of the corrosion products generated in water and $(\text{NH}_4)_2\text{SO}_4$ solutions (samples C₁ to C₂₄)

Sample	Phase composition (approximate molar fraction)
C ₁	$\gamma\text{-FeOOH} + \text{Fe}_3\text{O}_4$ (1/8)
C ₂	$\gamma\text{-FeOOH} + \text{Fe}_3\text{O}_4$ (1/6)
C ₃	$\gamma\text{-FeOOH} + \text{Fe}_3\text{O}_4$ (1/5)
C ₄	$\gamma\text{-FeOOH} + \text{Fe}_3\text{O}_4$ (1/4)
C ₅	$\gamma\text{-FeOOH} + \text{Fe}_3\text{O}_4$ (1/4)
C ₆	$\text{Fe}_3\text{O}_4 + \gamma\text{-FeOOH} + \alpha\text{-Fe}_2\text{O}_3$ (1/8) (1/20)
C ₇	$\text{Fe}_3\text{O}_4 + \gamma\text{-FeOOH} + \alpha\text{-Fe}_2\text{O}_3$ (1/8) (1/20)
C ₈	$\text{Fe}_3\text{O}_4 + \alpha\text{-Fe}_2\text{O}_3 + \gamma\text{-FeOOH}$ (1/10) (1/20)
C ₉	$\gamma\text{-FeOOH}$
C ₁₀	$\gamma\text{-FeOOH}$
C ₁₁	$\gamma\text{-FeOOH}$
C ₁₂	$\gamma\text{-FeOOH} + \text{Fe}_3\text{O}_4$ (1/8)
C ₁₃	$\text{Fe}_3\text{O}_4 + \gamma\text{-FeOOH} + \alpha\text{-FeOOH}$ (1/4) (1/4)
C ₁₄	$\alpha\text{-FeOOH} + \alpha\text{-Fe}_2\text{O}_3 + \text{Fe}_3\text{O}_4$ (1/10) (1/10)
C ₁₅	$\alpha\text{-FeOOH} + \alpha\text{-Fe}_2\text{O}_3 + \text{Fe}_3\text{O}_4$ (1/10) (1/10)
C ₁₆	$\alpha\text{-FeOOH} + \alpha\text{-Fe}_2\text{O}_3 + \text{Fe}_3\text{O}_4$ (1/4) (1/8)
C ₁₇	$\gamma\text{-FeOOH}^*$
C ₁₈	$\gamma\text{-FeOOH}^*$
C ₁₉	$\gamma\text{-FeOOH}^*$
C ₂₀	$\gamma\text{-FeOOH}^*$
C ₂₁	$\gamma\text{-FeOOH}$
C ₂₂	$\alpha\text{-Fe}_2\text{O}_3 + \gamma\text{-FeOOH}$ (1/3)
C ₂₃	$\alpha\text{-Fe}_2\text{O}_3 + \gamma\text{-FeOOH}$ (1/10)
C ₂₄	$\alpha\text{-Fe}_2\text{O}_3 + \alpha\text{-FeOOH} + \gamma\text{-FeOOH}$ (1/10) (1/20)

* Broadened diffraction lines

Remark: A small amorphous fraction may be a present in early stages of corrosion.

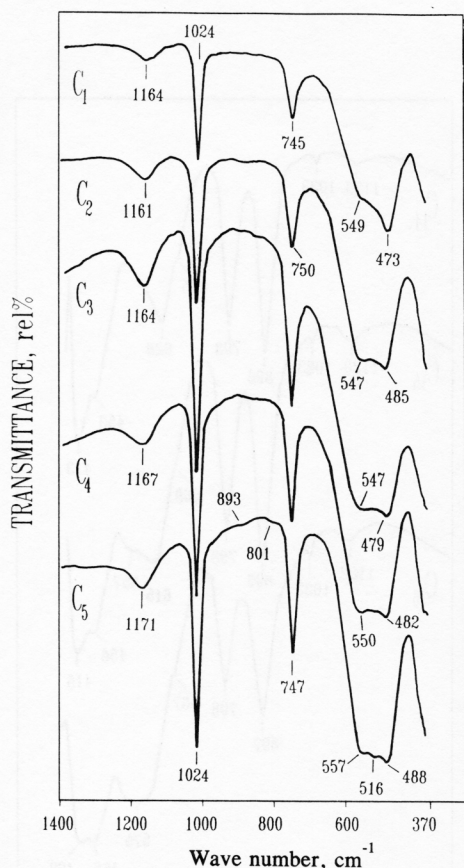


Figure 1. Fourier transform IR spectra of corrosion products C_1 to C_5 , recorded at room temperature.

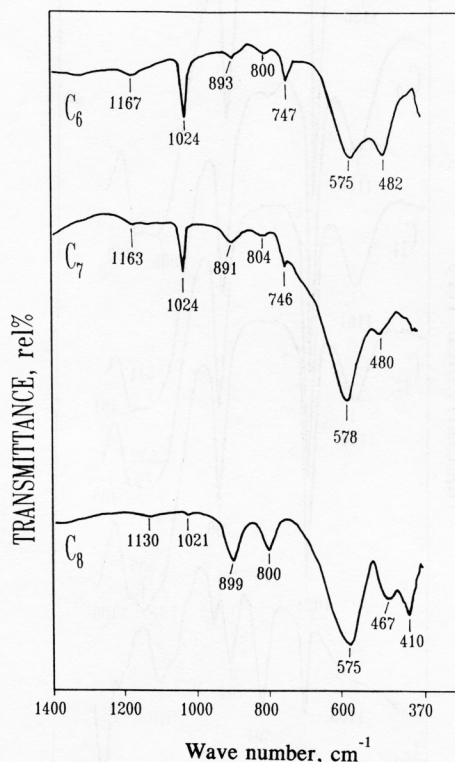


Figure 2. Fourier transform IR spectra of corrosion products C_6 to C_8 , recorded at room temperature.

Corrosion of steel in 0.1 M $(\text{NH}_4)_2\text{SO}_4$ solution at 20 °C, between 1 and 7 days, generated $\gamma\text{-FeOOH}$ as a single phase in the rust (samples C_9 to C_{11}), as shown by XRD (Table II). After 21 days of corrosion, Fe_3O_4 was detected by XRD as an additional component (sample C_{12}), while after 3 months of corrosion, besides Fe_3O_4 , $\gamma\text{-FeOOH}$ and $\alpha\text{-FeOOH}$ were present (sample C_{13}). FT-IR spectroscopic results obtained for samples C_9 to C_{13} (Figure 3) are in accordance with XRD results. A different phase composition of the rust was obtained when the corrosion of steel in 0.1 M $(\text{NH}_4)_2\text{SO}_4$ solution was performed at 90 °C. XRD analysis of samples C_{14} to C_{16} indicated that $\alpha\text{-FeOOH}$ was the dominant component in these samples, while $\alpha\text{-Fe}_2\text{O}_3$ and Fe_3O_4 were determined as additional components (Table II). FT-IR spectra of samples C_{14} to C_{16} (Figure 4) also showed that $\alpha\text{-FeOOH}$ prevailed in these samples, according to the bands at 896 and 798 cm^{-1} . A very weak peak at 1023–1022 cm^{-1} , due to a small amount of $\gamma\text{-FeOOH}$, was observed in FT-IR spectra of samples C_{14} to C_{16} .

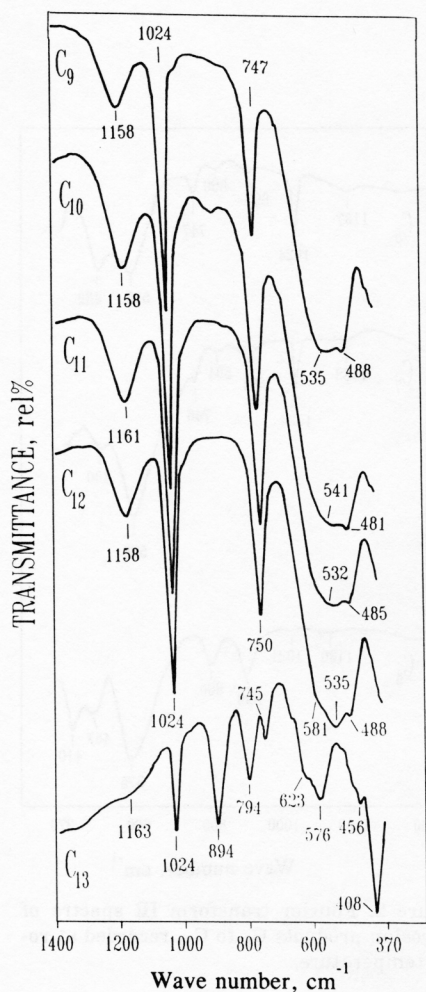


Figure 3. Fourier transform IR spectra of corrosion products C_9 to C_{13} , recorded at room temperature.

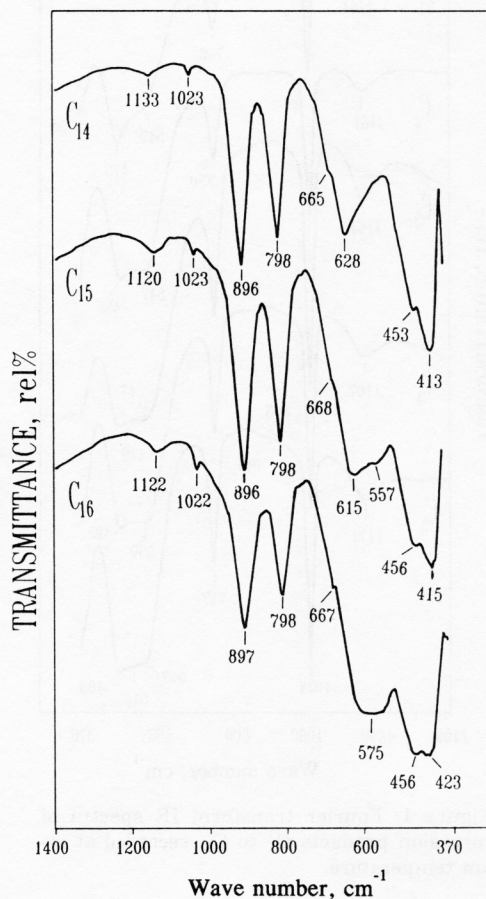


Figure 4. Fourier transform IR spectra of corrosion products C_{14} to C_{16} , recorded at room temperature.

Corrosion of steel in 2 M $(\text{NH}_4)_2\text{SO}_4$ solution at 20 °C, up to 3 months, generated γ -FeOOH as a single phase, samples C_{17} to C_{21} , (Table II). XRD lines of γ -FeOOH in samples C_{17} to C_{20} were broadened. FT-IR spectra of samples C_{17} to C_{21} , shown in Figure 5, also indicated the presence of γ -FeOOH. The presence of a small amount of α -FeOOH in sample C_{21} could be recognized on the basis of a band at 895 cm^{-1} and a shoulder at 795 cm^{-1} .

After corrosion of steel in 2 M $(\text{NH}_4)_2\text{SO}_4$ solutions at 90 °C, up to 3 days, α -Fe₂O₃ was determined by XRD as the main component and γ -FeOOH as an additional com-

ponent (samples C_{22} to C_{24}). XRD also showed the presence of α -FeOOH in sample C_{24} . FT-IR spectra of samples C_{22} to C_{23} are shown in Figure 6. On the basis of very strong bands at 537 – 550 cm^{-1} and 473 – 471 cm^{-1} , it was confirmed that α -Fe $_2$ O $_3$ is the dominant component in the rust. In sample C_{22} , the presence of γ -FeOOH was detected on the basis of bands at 1024 and 744 cm^{-1} , while α -FeOOH was detected on the basis of a band at 885 cm^{-1} and a shoulder at 794 cm^{-1} . With increased time of corrosion, the intensities of the bands at 1024 and 747 cm^{-1} , corresponding to γ -FeOOH, were decreased. In samples C_{23} and C_{24} , α -FeOOH was detected on the basis of bands at 896 and 800 cm^{-1} , and 898 and 802 cm^{-1} , respectively.

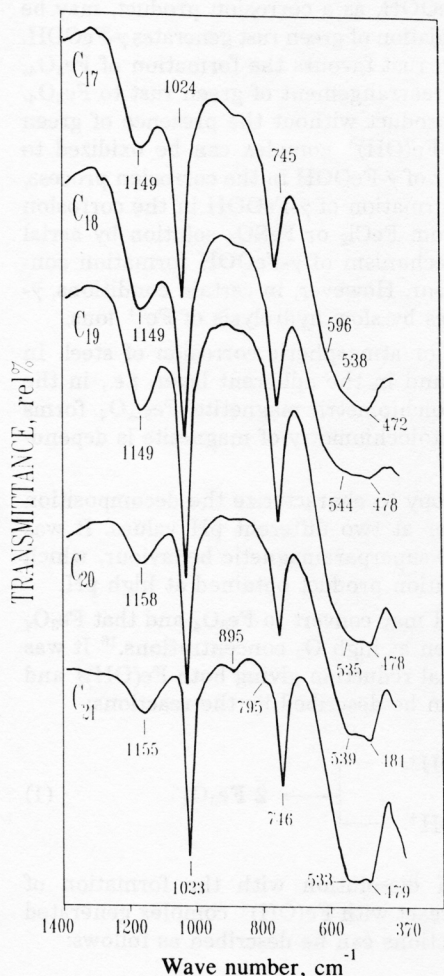


Figure 5. Fourier transform IR spectra of corrosion products C_{17} to C_{21} , recorded at room temperature.

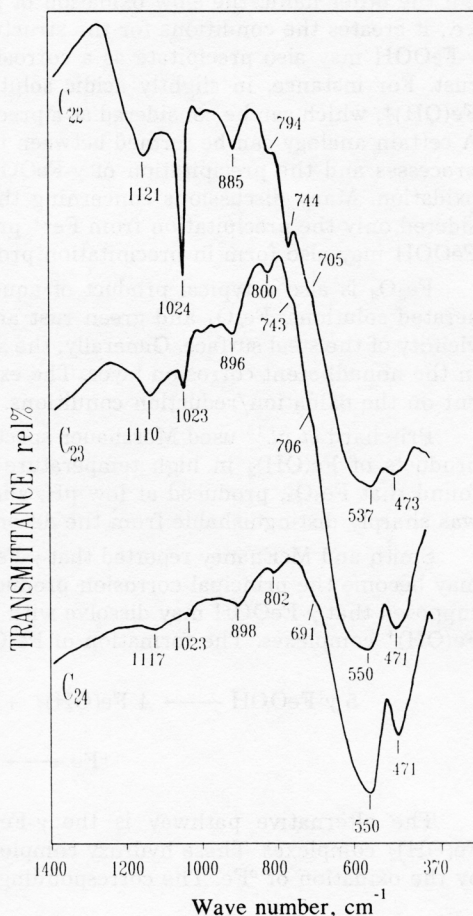


Figure 6. Fourier transform IR spectra of corrosion products C_{22} to C_{24} , recorded at room temperature.

DISCUSSION

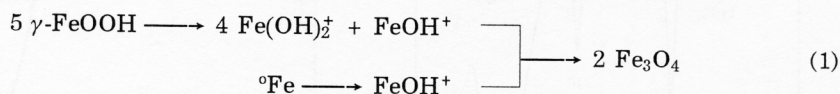
In the present work, four oxide phases, lepidocrocite (γ -FeOOH), goethite (α -FeOOH), magnetite (Fe_3O_4) and hematite (α - Fe_2O_3), were found in corrosion products. Their distribution or absence of some oxide phases in the corrosion products were dependent on the experimental conditions of the corrosion of steel. The experiments performed at 20 °C clearly demonstrated regularities in the phase composition of corrosion products. γ -FeOOH was the dominant component in the rust in all samples obtained at 20 °C, except for sample C₁₃, where Fe_3O_4 was dominant. Also, all samples, generated in doubly distilled water at 20 °C, up to 3 months, contained Fe_3O_4 , while for the same corrosion times in the samples generated in 2 M $(\text{NH}_4)_2\text{SO}_4$ solution Fe_3O_4 was not observed.

Many researchers found γ -FeOOH in the rust, particularly in the rust formed in early stages of the corrosion process.^{1,10-14} γ -FeOOH, as a corrosion product, may be formed by different pathways. The rapid aerial oxidation of green rust generates γ -FeOOH. On the other hand, the slow oxidation of green rust favours the formation of Fe_3O_4 , i.e., it creates the conditions for the structural rearrangement of green rust to Fe_3O_4 . γ -FeOOH may also precipitate as a corrosion product without the presence of green rust. For instance, in slightly acidic solution, $\text{Fe}(\text{OH})^+$ complex can be oxidized to $\text{Fe}(\text{OH})_2^+$, which can be considered as a precursor of γ -FeOOH in the corrosion process. A certain analogy can be formed between the formation of γ -FeOOH in the corrosion processes and the precipitation of γ -FeOOH from FeCl_2 or FeSO_4 solution by aerial oxidation. Many discussions concerning the mechanism of γ -FeOOH formation considered only the precipitation from Fe^{2+} precursor. However, in certain conditions, γ -FeOOH may also form in precipitation processes by slow hydrolysis of Fe^{3+} ions.

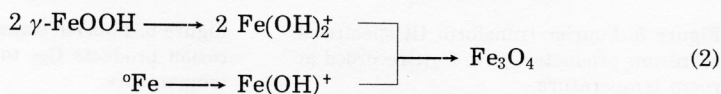
Fe_3O_4 is also a typical product of aqueous or atmospheric corrosion of steel. In aerated solutions, Fe_3O_4 and green rust are found in the adherent layer, i.e., in the vicinity of the steel surface. Generally, the substoichiometric magnetite, $\text{Fe}_{3-x}\text{O}_4$, forms in the nonadherent corrosion layer. The exact stoichiometry of magnetite is dependent on the oxidation/reduction conditions.

Pritchard *et al.*¹⁵ used Mössbauer spectroscopy to characterize the decomposition products of $\text{Fe}(\text{OH})_2$ in high temperature water at two different pH values. It was found that Fe_3O_4 , produced at low pH, showed superparamagnetic behaviour, which was sharply distinguishable from the decomposition product obtained at high pH.

Smith and McEnaney reported that γ -FeOOH may convert to Fe_3O_4 and that Fe_3O_4 may become the principal corrosion product even at high O_2 concentrations.¹⁶ It was supposed that γ -FeOOH may dissolve with partial reduction giving both $\text{Fe}(\text{OH})_2^+$ and $\text{Fe}(\text{OH})^+$ complexes. The formation of Fe_3O_4 can be described by the reactions:



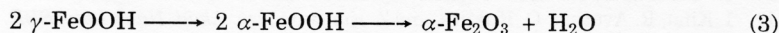
The alternative pathway is the γ -FeOOH dissolution with the formation of $\text{Fe}(\text{OH})_2^+$ complexes. These hydroxy complexes react with $\text{Fe}(\text{OH})^+$ complex generated by the oxidation of ${}^0\text{Fe}$. The corresponding reactions can be described as follows:



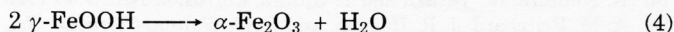
Kassim *et al.*¹⁷ found that the initial corrosion product of iron in aqueous environment was the green rust, which converted to γ -FeOOH or Fe_3O_4 depending on the oxidation rate, as well as on the concentration of dissolved oxygen. The transformation of the green rust to the Fe_3O_4 was explained by the solid state transformation. The process of transformation γ -FeOOH \longrightarrow Fe_3O_4 was also simulated by electrochemical methods.^{18,19}

The strong influence of $(\text{NH}_4)_2\text{SO}_4$ electrolyte on the formation of the rust and its phase composition can be considered as a cumulative effect of two aggressive ions, NH_4^+ and SO_4^{2-} . The presence of SO_4^{2-} ions, at given pH values, can create corrosion conditions that show a certain analogy with the processes of precipitation of iron oxyhydroxides and oxides from FeSO_4 solutions. On the other hand, the presence of NH_4^+ ions may promote the dissolution of iron (steel) into the solution,²⁰ thus accelerating the corrosion reactions. In 2 M $(\text{NH}_4)_2\text{SO}_4$ solution, Fe_3O_4 was not formed, even after 3 months of corrosion, in spite of the fact that pH conditions (Table I) favoured the formation of Fe_3O_4 .

In the rust formed in $(\text{NH}_4)_2\text{SO}_4$ solutions at room temperature, no significant amount of α -FeOOH was found. However, an opposite situation was found in the rust samples obtained at 90 °C, for instance in samples C₁₄ to C₁₆. According to the analysis of the rust, it may be concluded that γ -FeOOH is the main source of material for the formation of α -FeOOH. Very probably, this transformation occurred by a dissolution/reprecipitation mechanism. Generally, the transformation of γ -FeOOH to α -FeOOH and α -Fe₂O₃ can be expressed by the reactions:



and



At room temperature, the nucleation of α -FeOOH is easier than that of α -Fe₂O₃. With increase of temperature of aqueous medium the appearance of α -Fe₂O₃ in the rust is more probable and this effect is observed in the present study. At 90 °C, all corrosion reactions are very accelerated. The formation of α -FeOOH in a more significant amount at 90 °C, than at 20 °C, can be explained by an increased rate of γ -FeOOH dissolution and increased concentration of Fe^{3+} ions.

CONCLUSION

Four oxide phases, lepidocrocite (γ -FeOOH), goethite (α -FeOOH), magnetite (Fe_3O_4) and hematite (α -Fe₂O₃) were detected in the corrosion products formed by the corrosion of steel in doubly distilled water or $(\text{NH}_4)_2\text{SO}_4$ solutions. Their distribution or absence of some oxide phases in the corrosion products were dependent on the concentration of $(\text{NH}_4)_2\text{SO}_4$ solution, the temperature and the time of corrosion. Fourier transform IR spectroscopy, which was used as a complementary technique to X-ray diffraction, was particularly useful in detection of small amounts of γ -FeOOH and α -FeOOH. γ -FeOOH was the dominant component in all corrosion products obtained at 20 °C, except for one sample where Fe_3O_4 was dominant. All corrosion products generated in doubly distilled water at 20 °C, up to 3 months, contained Fe_3O_4 , while for the same corrosion times, Fe_3O_4 was not detected in the samples obtained in 2 M $(\text{NH}_4)_2\text{SO}_4$.

solutions. The formation of $\alpha\text{-Fe}_2\text{O}_3$ phase was observed only at 90 °C. The strong influence of $(\text{NH}_4)_2\text{SO}_4$ electrolyte on the corrosion of steel in aqueous medium can be explained as a cumulative effect of two aggressive ions, NH_4^+ and SO_4^{2-} . The presence of SO_4^{2-} ions, at given pH values, created corrosion conditions that showed a certain analogy with the processes of precipitation of iron oxyhydroxides and oxides from FeSO_4 solutions. On the other hand, the presence of NH_4^+ ions may promote the dissolution of iron (steel) into the solution, thus accelerating the corrosion reactions.

Acknowledgements. — We thank Dr. Mira Ristić and Mr. Goran Štefanić for technical assistance during the preparation of the manuscript.

REFERENCES

1. H. Leidheiser, Jr. and S. Musić, *Corrosion Sci.* **22** (1982) 1089.
2. H. Leidheiser, Jr., S. Musić, and J. F. McIntyre, *ibid.* **24** (1984) 197.
3. S. Musić, A. Vértés, G. W. Simmons, I. Czakó-Nagy, and H. Leidheiser, Jr., *J. Colloid Interface Sci.* **58** (1982) 256.
4. S. Musić, I. Czakó-Nagy, S. Popović, A. Vértés, and M. Tonković, *Croat. Chem. Acta* **59** (1986) 833.
5. S. Musić, S. Popović, and M. Gotić, *ibid.* **60** (1987) 661.
6. S. Musić, S. Popović, and M. Gotić, *J. Mater. Sci.* **25** (1990) 3186.
7. S. Musić, S. Popović, and M. Ristić, *ibid.* **28** (1993) 632.
8. S. Musić, M. Gotić, and S. Popović, *ibid.* **28** (1993) 5744.
9. S. Musić, Z. Orehovec, S. Popović, and I. Czakó-Nagy, *ibid.* in press.
10. H. Leidheiser, Jr. and I. Czakó-Nagy, *Corrosion Sci.* **24** (1984) 569.
11. I. Kina, R. Avotina, O. Kukurs, and Z. Konstans, *Izv. Akad. Nauk Latv. SSR, Ser. Khim.* (1983) 281.
12. H. V. Varma and M. Mathur, *Bull Electrochem.* **6** (1990) 747.
13. G. Belozerskii, C. Bohm, T. Ekdahl, and D. Liljequist, *Corrosion Sci.* **22** (1982) 831.
14. K. Nomura, M. Tasaka and Y. Ujihira, *Corrosion NACE* **44** (1988) 131.
15. A. M. Pritchard, J. R. Haddon, and G. N. Walton, *Corrosion Sci.* **11**(1971) 11.
16. D. C. Smith and B. McEnaney, *ibid.* **19** (1979) 379.
17. J. Kassim, T. Baird, and J. R. Fryer, *ibid.* **22** (1982) 147.
18. M. Stratmann and K. Hoffmann, *ibid.* **29** (1989) 1329.
19. A. Kuch, *ibid.* **28** (1988) 221.
20. P. C. Bhat, M. P. Sathyavathiamma, N. G. Puttaswamy, and R. M. Mallya, *ibid.* **23** (1983) 733.

SAŽETAK

Stvaranje hrđe tijekom korozije čelika u vodi i otopinama $(\text{NH}_4)_2\text{SO}_4$

S. Musić, D. Dragčević i S. Popović

Stvaranje hrđe tijekom korozije čelika u vodi i otopinama $(\text{NH}_4)_2\text{SO}_4$ istraživano je do tri mjeseca pri 20 °C i do tri dana pri 90 °C.

Dobiveni korozijski produkti analizirani su primjenom difrakcije X-zraka i FT-IR spektroskopije. U korozijskim produktima detektirane su četiri oksidne faze; lepidokrokrit ($\gamma\text{-FeOOH}$), getit ($\alpha\text{-FeOOH}$), magnetit (Fe_3O_4) i hematit ($\alpha\text{-Fe}_2\text{O}_3$). Raspodjela tih faza ili odsutnost neke oksidne faze u korozijskim produktima izrazito je ovisila o eksperimentalnim uvjetima korozije čelika. Snažan utjecaj koncentracije $(\text{NH}_4)_2\text{SO}_4$ na fazni sastav hrđe objašnjen je kumulativnim efektom dvaju agresivnih iona (u korozijskom smislu), NH_4^+ i SO_4^{2-} . U radu su razmotreni i mogući mehanizmi stvaranja oksidnih faza u hrđi.